

On the plasma flow inside magnetic tornadoes on the Sun

Sven WEDEMEYER

Institute of Theoretical Astrophysics, University of Oslo, Postboks 1029 Blindern, N-0315 Oslo, Norway
sven.wedemeyer@astro.uio.no

Oskar STEINER

Kiepenheuer-Institut für Sonnenphysik, Schöneckstrasse 6, 79104 Freiburg i.Br., Germany
Istituto Ricerche Solari Locarno, Via Patocchi 57, 6605 Locarno-Monti, Switzerland
steiner@kis.uni-freiburg.de

(Received 2014 February 17; accepted 2014 June 26)

Abstract

High-resolution observations with the Swedish 1-m Solar Telescope (SST) and the Solar Dynamics Observatory (SDO) reveal rotating magnetic field structures that extend from the solar surface into the chromosphere and the corona. These so-called magnetic tornadoes are primarily detected as rings or spirals of rotating plasma in the Ca II 854.2 nm line core (also known as chromospheric swirls). Detailed numerical simulations show that the observed chromospheric plasma motion is caused by the rotation of magnetic field structures, which again are driven by photospheric vortex flows at their footpoints. Under the right conditions, two vortex flow systems are stacked on top of each other. We refer to the lower vortex, which extends from the low photosphere into the convection zone, as intergranular vortex flow (IVF). Once a magnetic field structure is co-located with an IVF, the rotation is mediated into the upper atmospheric layers and an atmospheric vortex flow (AVF, or magnetic tornado) is generated. In contrast to the recent work by Shelyag et al., we demonstrate that particle trajectories in a simulated magnetic tornado indeed follow spirals and argue that the properties of the trajectories decisively depend on the location in the atmosphere and the strength of the magnetic field.

Key words: convection, magnetohydrodynamics (MHD), Sun: atmosphere, Sun: magnetic fields

1. Introduction

High-resolution observations with the Swedish 1-m Solar Telescope (SST, Scharmer et al. 2003) in 2008 lead to the discovery of ‘chromospheric swirls’, which are seen as dark rings or spirals in the core of the Ca II infrared triplet line at a wavelength of 854.2 nm (Wedemeyer-Böhm & Rouppe van der Voort 2009). Subsequent observations with the SST and the Atmospheric Imaging Assembly (AIA) onboard the Solar Dynamics Observatory (SDO, Lemen et al. 2012) revealed that these swirls also have an imprint in the transition region and corona and that they, at the same time, are connected to magnetic bright points in the photosphere below (Wedemeyer-Böhm et al. 2012, hereafter Paper I). These observations were explained in Paper I with the help of numerical simulations, which have been carried out with the 3-D radiation magnetohydrodynamics codes CO⁵BOLD (Freytag et al. 2012) and Bifrost (Gudiksen et al. 2011). The simulations revealed that the observed chromospheric plasma motion is the result of rotating magnetic field structures, which are rooted in the top layers of the convection zone and extend throughout the atmosphere. When the photospheric footpoint and its highly conductive sub-photospheric part coincide with a photospheric vortex flow, then such a vortex causes the entire field structure to rotate because of the well satisfied frozen-in condition. The magnetic field effectively couples the atmospheric layers with each other and thus mediates

the rotation into the chromosphere, transition region, and corona. The visualisation of the simulated velocity field in a single instant of time produces spiraling streamlines, which remind of terrestrial tornadoes and hence led to the name (solar) “magnetic tornadoes”. These events may provide an alternative way of channeling energy and possibly matter into the upper solar atmosphere but many details and the resulting net contribution to heating the solar corona have yet to be investigated.

We focus here on these small-scale vortex flows in the photosphere and chromosphere and do not address rotating magnetic field structures, which are observed on larger spatial scales. The largest examples, here referred to as giant solar tornadoes are likely the rotating legs of solar prominences (e.g., Su et al. 2012; Li et al. 2012; Orozco Suárez et al. 2012; Wedemeyer et al. 2013a), but it is currently not clear if and how they are related to the small-scale events discussed here.

Recently, Shelyag et al. (2013) claimed that magnetic field concentrations in the solar photosphere do neither produce magnetic tornadoes nor a “bath-tub” effect. Here, we demonstrate that, contrary to the claims by Shelyag et al., the simulations presented in Paper I also show spiral-like particle trajectories when considering the full temporal resolution of the velocity field. We begin with the introduction and definition of different types of vortex flow in Sect. 2 and analyse particle trajectories based on the simulations from Paper I in Sect. 3. A

discussion of the results and conclusions are presented in Sect. 4.

2. Different types of vortex flow

First, we would like to emphasise that there are several types of vortex flows that occur on the Sun. The formation of a vortex flow in the photosphere is a direct consequence of the conservation of angular momentum carried by plasma, which sinks down from the surface into the upper convection zone. Consequently, a vortex flow is produced, which extends into the upper layers of the convection zone. This hydrodynamic process is also known as bathtub effect (cf. Sect. 3.3 in Nordlund 1985) because it resembles the swirling water in the sink of a bathtub. The effect is most pronounced at the vertices of intergranular lanes, where plasma from neighbouring granules converges (see also, e.g., Porter & Woodward 2000; Kitiashvili et al. 2012). Such flow systems are an integral part of stellar surface convection. We will refer to this phenomenon as intergranular vortex flow (IVF) hereafter. This phenomenon, which is essentially known since the beginnings of hydrodynamic simulations of the solar surface layers, has also been called ‘inverted tornado’ by Nordlund (1985). IVFs are also very abundant in the simulations by Moll et al. (2011) who find vortices with nearly vertical orientation predominantly in intergranular lanes. They present an example with a horizontal diameter of approximately 80 km, which corresponds to 0.1 arcsec and would thus be difficult to observe with currently available telescopes. However, photospheric vortex flows have been observed on different spatial scales and can be much larger than an intergranular lane (e.g., Brandt et al. 1988; Bonet et al. 2008, 2010; Vargas Domínguez et al. 2011). Moll et al. (2011) suggest that some granular-scale vortices could be the peripheral parts of strong but unresolved small-scale vortex flows, i.e. IVFs.

In the presence of magnetic fields, another type of vortex flow can develop in the atmospheric layers above an IVF if the foot point of a magnetic field structure coincides locally with an IVF. The small-scale atmospheric vortex flows, which are produced in this way, have been named magnetic tornado in Paper I and are referred to as AVFs hereafter in order to more clearly distinguish them from IVFs.

The two different types of vortex flow are illustrated in Fig. 1. Each AVF is driven by an IVF, although IVFs can obviously exist without a corresponding AVF. The ratio of thermal gas pressure to magnetic pressure, i.e., plasma- β , is large in the upper convection zone of quiet Sun regions. There, the gas is significantly ionized so that the magnetic field is essentially frozen-in and is advected with the convective flows. Consequently, the magnetic field is forced to co-rotate with the plasma flow inside an IVF, which results in the rotation of the magnetic footpoint and with it in the rotation of the entire magnetic field structure. A pronounced AVF only develops if the photospheric footpoint of the corresponding magnetic field structure is co-located with the IVF long enough. As already suggested

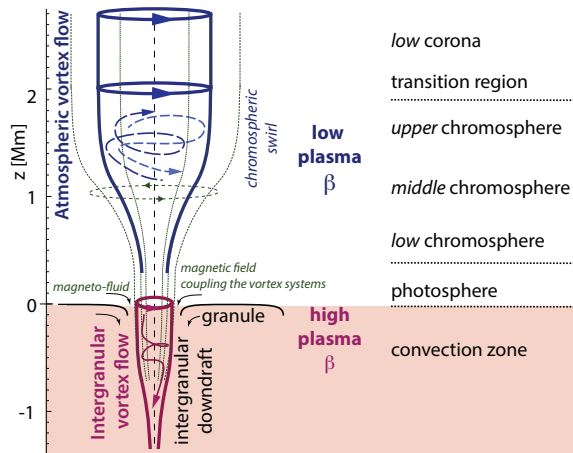


Fig. 1. Schematic double-nature of vortex flows. An atmospheric vortex flow (AVF), also known as ‘magnetic tornado’ as introduced in Paper I can exist on top of a photospheric intergranular vortex flow (IVF), which extends into the upper convection zone and drives the AVF above. The virtual boundaries of both vortex flows are illustrated with thick solid lines. In the AVF plasma can propagate upwards and downwards (thin lines with arrows), while plasma sinks down in the IVF below. The AVF forms under low plasma- β conditions, whereas the IVF is located in the denser lower layers with a high plasma- β . Both vortex flows are coupled together by the magnetic field (thin line). The depicted vortex system is idealised and has a vertically aligned axis and magnetic field structure, IVF, and AVF being aligned. In general, the axis can be tilted and curved, depending on the magnetic field at this location.

by Wedemeyer et al. (2013b), it can happen that the magnetic footpoint is moving only temporarily into the IVF or that the IVF is decaying, which then results in only a partial rotation of the magnetic field in the atmosphere and thus not in a fully developed AVF. A continuous spectrum from partial to full rotation events can be expected. In Paper I, it was shown that these rotating magnetic field structures have detectable observational imprints in the chromosphere (‘swirls’) and in many cases in the corona above. Although the detection of chromospheric swirls has been near the observational limit so far, it should be possible to derive a more comprehensive picture of the full spectrum of swirls regarding, e.g., lifetimes and number of full revolutions in the near future with upcoming new, more powerful solar telescopes such as the 4-m Daniel K. Inouye Solar Telescope (DKIST, formerly the Advanced Technology Solar Telescope, ATST Keil et al. 2011) and the 4-m European Solar Telescope (EST Collados et al. 2010).

The distinction between IVFs and AVFs can also be understood in view of the different plasma conditions, under which they occur. IVFs are produced at the interface between the dense upper convection zone and the photosphere, where plasma- β is large. Here, the plasma dominates and drags the magnetic field with it. In contrast, an AVF forms in the atmosphere in a low plasma- β environment under the influence of a driving IVF below. Here, the magnetic field dominates and drags the plasma with it. The thick solid lines in Fig. 1 illustrate the spa-

tial extent of both vortex systems. The lines are by no means solid barriers. Rather, plasma and associated magnetic field can join and leave the vortex system from all sides at all times, which renders the magnetic field structure more complicated than can be sketched in the simplified cartoon. An impression of this complexity is given in Fig. 2. Inside the vortex flows, plasma particles can propagate downwards and upwards, although they are mostly dragged downwards in an IVF. Being coupled by the rotating magnetic field structure, plasma can propagate between the two vortex systems but we find that the flow speeds in the upper photosphere are much smaller than in the individual vortex flows above and below. Rather than of a rigid magnetic flux tube with impenetrable boundaries, one should think of this flux system as a magneto-fluid in which local magnetic flux concentrations are part of a continuous magnetic flux distribution, i.e. part of a continuous magneto-fluid. Material from the lateral granular flow can penetrate and deform the photospheric flux concentration and thus lead to downdrafts within it.

Moll et al. (2011) provide a further definition and classification of vortices based on the so-called ‘swirling strength’ (Zhou et al. 1999) and distinguish between mostly vertical and horizontally orientated vortices. The vortex flows discussed in this section so far are orientated vertically and therefore different from the horizontal vortex tubes reported by Steiner et al. (2010), which are found at the edges of granules both in simulations and observations.

Vortex motions in the atmosphere can also be driven by the rapid unwinding of twisted magnetic fields instead of the bathtub effect, as it is observed in prominence eruptions (e.g., Su & van Ballegoijen 2013; Yan et al. 2013). This unwinding process is different from the convective vortex driving discussed here.

3. Particle trajectories

The numerical simulation presented in Paper I consists of a sequence of CO⁵BOLD model snapshots with a cadence of 1 s, which is part of a much longer simulation run. In Paper I, the velocity field is visualized in the form of *instant* streamlines, which trace the flow field for selected snapshots starting from a set of seed points. A similar visualisation of the flow field is shown in Fig. 2. These streamlines must not be confused with actual particle trajectories because the velocity field evolves while a particle propagates. Any particle starting from a point on one of the plotted streamlines would follow the streamline in good approximation for a short time so that streamlines still give a good overall impression of the propagation of particle ensembles within such a flow system. The true trajectory of an *individual* particle, however, would deviate from the initial streamline after a short time. True particle trajectories had not been shown in Paper I but do also exhibit spirals, which can be seen here in Fig. 3. The trajectories are calculated by following a large number of test particles from their seed points in each grid cell of the depicted sub-domain through the time sequence of

snapshots with 1 s cadence and subsequent refinement to 0.1 s. The considered sequence is 5 min long. For clarity, only about 1000 representative trajectories are plotted.

The three-dimensional visualisation of the particle trajectories again gives a tornado-like impression. Extremely curved and spiral-like particle tracks can be seen in both the chromosphere in the upper part of the domain and in the convection zone below. Individual particles, however, may enter and leave the tornado-like region while others perform one or several full revolutions around the vortex axis. The radius of the particle spirals corresponds to the size of observed chromospheric swirls in the upper part of the domain, while the radius is much smaller in the convection zone. The side view (bottom panel in Fig. 3) reveals that essentially no particle is travelling the full height range of the tornado during the relatively short duration of the considered sequence. It appears almost as if the flows above and below the middle photosphere are disconnected although both remain of course tightly coupled by the magnetic field. Particles, which start from below the middle photosphere, spiral downwards into the IVF, while particles, which start above the photosphere, remain in the atmosphere and follow the AVF there. The particles, which start in the photosphere and below, travel downwards into the IVF with absolute velocities $|\vec{v}|$ of up to 10.0 km s^{-1} and an average of $(4.6 \pm 2.0) \text{ km s}^{-1}$. Particles, which start from positions above the photosphere, can propagate both upwards and downwards in the AVF and can also change the vertical direction on the way through the vortex. The maximum absolute speed $|\vec{v}|$ of the considered particles reaches 24.5 km s^{-1} , with a mean of $(13.3 \pm 4.0) \text{ km s}^{-1}$. The corresponding vertical velocity component v_z ranges from -17.0 km s^{-1} to 19.0 km s^{-1} (where negative velocities indicate downdrafts). An AVF would therefore most likely drain material from the chromosphere, which possibly results in a net mass transport into the corona.

The *apparent* ‘gap’ between the flow systems, which is located in the (upper) photosphere, lays in between two different physical regimes: the high plasma- β lower layers and the low plasma- β upper layers. The magnetic field is “frozen-in” in both regimes. However, while the plasma dominates and advects magnetic field with the convective flows in the lower part (i.e., in the IVF) it is vice versa in the upper part, i.e., in the AVF. There, the magnetic field dominates and is forcing the plasma flows, resulting in the observed chromospheric swirls. The ionization degree is lowest in the photosphere so that the magnetic field is not frozen-in perfectly in the apparent “gap”, which is nevertheless permeated by the rotating magnetic field. An IVF is essentially a hydrodynamic phenomenon because it occurs in the high plasma- β regime. It can also be (partially) field free and can have a large region of influence from where plasma can be dragged into the vortex. This way also additional magnetic field can be swept into the vortex and be added to the rotating magnetic field structure, which is eventually driving the AVF in the chromosphere above.

It should be noted that the magnetic field in the sim-

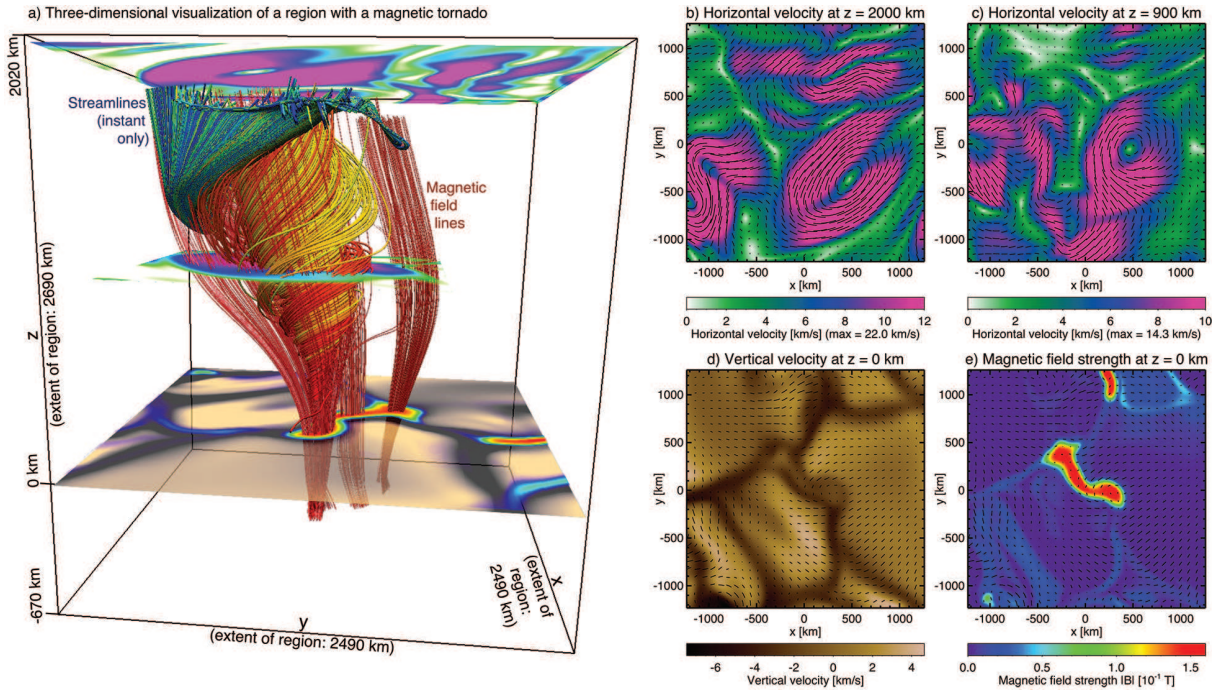


Fig. 2. Visualisation of a close-up region in the numerical model by Wedemeyer-Böhm et al. (2012) exhibiting a magnetic tornado. The (red) mostly vertical lines in panel a) represent the magnetic field, whereas the spiral lines (red-yellow-green-blue) represent the instant streamlines of the plasma in the magnetic tornado. The lower plane shows the granulation pattern of the solar surface at a height $z = 0$ km (grey-yellowish shades) overlaid with the magnetic footpoints (blue-green-red), whereas the swirl signature (pink ring) can be seen on the top ($z = 2000$ km) and at an intermediate level ($z = 900$ km). Please note that the displayed magnetic field lines and streamlines only refer to a single instant in time. The magnetic field rotates in time and the velocity field evolves, too. Consequently, individual (charged) particles do not cross any magnetic field line but do follow the rotating magnetic field lines. The resulting trajectories are shown in Fig. 3. This image was produced with VAPOR (Clyne & Rast 2005; Clyne et al. 2007). The planes are shown in more detail in panels b-e: b) Horizontal velocity at $z = 2000$ km, c) horizontal velocity at $z = 900$ km, d) vertical velocity at $z = 0$ km (with negative velocities for downflows), and e) absolute magnetic field strength at $z = 0$ km, all overlaid with streamlines rendering the horizontal flow field in that instant of time.

Table 1. Comparison of different numerical simulations, which exhibit vortex flows in the low photosphere. The following radiation magnetohydrodynamics codes are used: CO⁵BOLD (Freytag et al. 2012), SolarBox (Jacoutot et al. 2008), MuRAM (Vögler et al. 2005), and Bifrost (Gudiksen et al. 2011)

Reference	MHD code	Initial magnetic field $ B _0$	Height of lower boundary	Height of upper boundary
Freytag et al. (2012)	CO ⁵ BOLD	0 G	-2400 km	2000 km
Kitiashvili et al. (2011)	SolarBox	0 G	-5000 km	500 km
Kitiashvili et al. (2013)	SolarBox	0 G	-5200 km	1000 km
Moll et al. (2012)	MuRAM	0 G	-900 km	800 km
Steiner & Rezaei (2012)	CO ⁵ BOLD	0 G	-1400 km	1400 km
Kitiashvili et al. (2013)	SolarBox	10 G	-5200 km	1000 km
Carlsson et al. (2010)	Bifrost	40 G	-1400 km	14100 km
Steiner & Rezaei (2012)	CO ⁵ BOLD	50 G	-1400 km	1400 km
Wedemeyer-Böhm et al. (2012)	CO ⁵ BOLD	50 G	-2400 km	2000 km
Moll et al. (2012)	MuRAM	200 G	-900 km	800 km
Shelyag et al. (2013)	MuRAM	200 G	-800 km	600 km

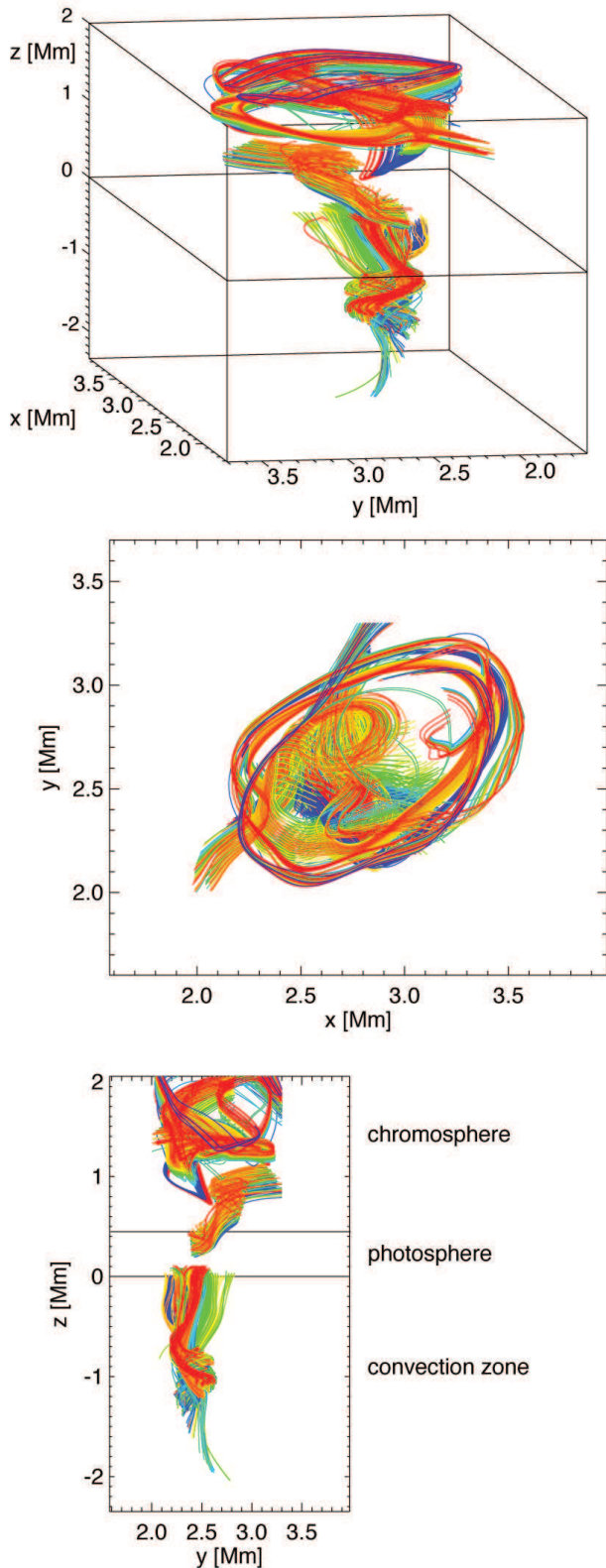


Fig. 3. About 1000 representative particle trajectories in the numerical model of the magnetic tornado shown in Fig. 2 (see also Paper I). The selected trajectories differ in colour/grey scale and are plotted for different perspectives: Three-dimensional (top), top view down (middle), and from the side (bottom).

ulation (mostly vertical lines in Fig. 2, red in the online version) is hardly twisted throughout the modelled atmospheric layers, i.e., in the computational domain above optical depth unity. The model atmosphere extends to only 2 Mm, which is small compared to the spatial scales over which significant twist is to be expected in this low plasma- β regime.

4. Discussion and conclusions

Visualisations of the velocity field exhibit clear spiral streamlines in the simulations by Moll et al. (2012), Wedemeyer-Böhm et al. (2012), Kitiashvili et al. (2013), and Shelyag et al. (2013). These simulations all started by superimposing a homogeneous vertical magnetic field on a relaxed simulation snapshot of solar surface convection but differ in terms of spatial extent, initial magnetic field strength and numerical details. Spiral streamlines are also found in the models by Moll et al. (2011), which were started with weak and initially random magnetic fields. Photospheric vortex flows occur also in the hydrodynamic simulations by Kitiashvili et al. (2011) and the simulation run v50 by Steiner & Rezaei (2012) with an initially homogeneous magnetic vertical field with $|B|_0 = 50$ G. Swirling motions are observed in the model by Carlsson et al. (2010), which was calculated with Bifrost (Gudiksen et al. 2011). They suggest that the presented swirl is produced by acoustic waves travelling upwards along twisted magnetic field lines (see also the Supplementary Information in Paper I). Furthermore, Moll et al. (2012) and Kitiashvili et al. (2013) provide a non-magnetic simulation for comparison. The non-magnetic model, from which the simulation by Wedemeyer-Böhm et al. (2012) was started, is illustrated in Freytag et al. (2012). Some properties of all aforementioned simulations, which are relevant for the discussion here, are summarised in Table 1.

The models extend to different heights in the atmosphere. The model by Wedemeyer-Böhm et al. (2012) includes the upper chromosphere up to 2 Mm, while Kitiashvili et al. (2013) put the upper boundary at a height of 1 Mm in the middle chromosphere. The simulations by Moll et al. (2012), which were calculated with the MURaM code (Vögler et al. 2005), reach up to a height of 800 km, i.e. into the low chromosphere. The model by Shelyag et al. (2013), which was calculated with the MURaM code, too, has a comparatively small total height extent of only 1.4 Mm. Their upper boundary is located at only 600 km height and thus barely above the photosphere and the classical temperature minimum region and lacks the layers where the observable imprint of magnetic tornadoes, i.e. chromospheric swirls, is formed. For comparison, the onset of shock formation, which is an important structuring agent of the chromosphere, only occurs above 700-800 km (e.g., Carlsson & Stein 1995; Wedemeyer et al. 2004). The model by Shelyag et al. (2013) thus cannot be used to make conclusions about the solar chromosphere and vortex flows therein.

Furthermore, the numerical simulations by Shelyag et al. (2013) started with a uniform vertical magnetic

field with a magnetic field strength of $|B|_0 = 200$ G superimposed on a developed non-magnetic model. After an initial phase of 40 min solar time, they write out model snapshots with a cadence of 2.41 s, which are then used for the calculation of trajectories, similar to what has been presented in Sect. 3 of the present paper. Shelyag et al. (2013) also find swirls in their model, although at much lower heights in the solar photosphere. However, they report that the corresponding trajectories of test particles based on their simulation do not show any spirals and therefore do not have a tornado-like appearance. Shelyag et al. argue that the particles instead follow oscillatory trajectories, for which the magnetic tension in the intergranular downflows would play a decisive role. They conclude that the horizontal motions in their magnetic field structure are to be interpreted as torsional Alfvén waves. Shelyag et al. finally claim that spiral trajectories (like those reported in Paper I) were only present when visualising the velocity field of a single model snapshot and that they were absent when considering the particle tracks, which incorporate the temporal evolution of the velocity field.

In Sect. 3, we demonstrate to the contrary that the simulations from Paper I, which started with an initial magnetic field of $|B|_0 = 50$ G, do show spiral-like particle trajectories when considering the full temporal resolution of the velocity field. The most pronounced spirals in the streamlines within a single snapshot (see Fig. 2) are seen in the chromospheric part of the magnetic field structure, i.e. inside the AVF. The model by Shelyag et al. has its upper boundary at only $z = 600$ km and thus does not extend into this layer and can therefore not contain an AVF. The spiral trajectories in the simulated AVF appear most clearly at heights above $z \sim 700$ km, i.e. only at chromospheric heights, which are not included in the model by Shelyag et al. (2013). The chromospheric origin of AVFs is clear from observations of chromospheric swirls, which can only be seen in chromospheric diagnostics such as in narrow-band images taken in the core of spectral lines of singly ionised calcium. However, despite the difference in magnetic field strength, the particle trajectories in the model by Shelyag et al. (2013) may rather be compared to the particles in our IVF as seen in Fig. 3. There, the trajectories in the upper convection zone are much less extremely wound than the chromospheric trajectories inside the AVF above. Consequently, the particle trajectories in the lower part of the simulation by Wedemeyer-Böhm et al. (2012) are not in contrast to what is reported by Shelyag et al., while the corresponding streamlines in Fig. 2 and particle trajectories in Fig. 3 nevertheless exhibit pronounced spiral tracks in the atmosphere above.

The conclusions made by Shelyag et al. (2013) can also directly be compared to the work by Moll et al. (2012) because both use the MuRAM code and use an initial magnetic field with $|B|_0 = 200$ G. Moll et al. present a counter-rotating pair of vortex flows with clear spiral streamlines but unfortunately no particle trajectories. However, their simulations also suggest that the formation of vortex flows is an integral part of solar convection with important im-

plications for the dynamics, structure and heating of the atmospheric layers.

It should be emphasised that the magnetic tornadoes described in Paper I and here are not stationary. Instead, the central axis of the flow system, which corresponds to the vortex tube cores reported by Kitiashvili et al. (2013), is changing in time, deforms and sways back and forth. At the same time, particles move up and down in spirals around the central axis. The boundary of such a tornado-like flow system is not always sharply defined. Particles can enter and leave the “tornado” at different heights. These effects have to be taken into account for a meaningful visualisation of the complicated flow field.

Furthermore, it is plausible that properties like the abundance and strength of magnetic tornadoes, i.e. the part visible as chromospheric swirls, depend on the magnetic field strength and its topology and can thus be expected to vary between different regions on the Sun. The bathtub effect is an integral part of non-magnetic or weakly magnetised flows in the surface layers of the Sun and other stars but may eventually be impeded by magnetic fields above a certain field strength or of complicate topology. The correspondingly low plasma- β conditions may then hinder the plasma flow near the solar surface to rotate magnetic foot points. A comparison between simulations without and with weak field show that already an initial magnetic field of more than $|B|_0 = 10$ G can change the appearance of the chromosphere significantly. The otherwise dominant chromospheric shock wave pattern (e.g. Skartlien et al. 2000; Wedemeyer et al. 2004) is gradually suppressed and dynamics and structure are instead governed by shear and vortex flows in connection with magnetic field concentrations (cf. Moll et al. 2012; Steiner & Rezaei 2012; Kitiashvili et al. 2013). In this sense, the initial magnetic field strength of 200 G used by Shelyag et al. (2013) is already high and not representative for the regions where chromospheric swirls have been detected on the Sun. Therefore we caution any conclusion regarding chromospheric swirls based on these simulations alone. Finally, the existence of torsional Alfvén waves and their possible role for the energy transport within a magnetic tornado had been suggested already by Wedemeyer-Böhm et al. (2012) and is in no way in contradiction to tornado-like flows with spiral particle trajectories. A more systematic grid of numerical simulations with different magnetic field strengths and corresponding observations is needed to shed light on the detailed properties of vortex flows in the solar atmosphere.

The authors acknowledge support by the Research Council of Norway, grants 221767/F20 and 208026/F50.

References

- Bonet, J. A., Márquez, I., Sánchez Almeida, J., Cabello, I., & Domingo, V. 2008, *ApJL*, 687, L131

- Bonet, J. A., Márquez, I., Sánchez Almeida, J., et al. 2010, *ApJL*, 723, L139
- Brandt, P. N., Scharmer, G. B., Ferguson, S., Shine, R. A., & Tarbell, T. D. 1988, *Nature*, 335, 238
- Carlsson, M., Hansteen, V. H., & Gudiksen, B. V. 2010, *Mem. Soc. Astron. Italiana*, 81, 582
- Carlsson, M. & Stein, R. F. 1995, *ApJL*, 440, L29
- Clyne, J., Mininni, P., Norton, A., & Rast, M. 2007, *New J. Phys.*, 9, 1
- Clyne, J. & Rast, M. 2005, in *Proceedings of Visualization and Data Analysis 2005*, ed. J. C. G. M. T. B. K. Edited by Erbacher, Robert F.; Roberts, 284–294
- Collados, M., Bettonvil, F., Cavaller, L., et al. 2010, *Astronomische Nachrichten*, 331, 615
- Freytag, B., Steffen, M., Ludwig, H.-G., et al. 2012, *Journal of Computational Physics*, 231, 919
- Gudiksen, B. V., Carlsson, M., Hansteen, V. H., et al. 2011, *A&A*, 531, A154
- Jacoutot, L., Kosovichev, A. G., Wray, A. A., & Mansour, N. N. 2008, *ApJ*, 682, 1386
- Keil, S. L., Rimmele, T. R., Wagner, J., Elmore, D., & ATST Team. 2011, in *Astronomical Society of the Pacific Conference Series*, Vol. 437, *Solar Polarization 6*, ed. J. R. Kuhn, D. M. Harrington, H. Lin, S. V. Berdyugina, J. Trujillo-Bueno, S. L. Keil, & T. Rimmele, 319
- Kitiashvili, I. N., Kosovichev, A. G., Lele, S. K., Mansour, N. N., & Wray, A. A. 2013, *ApJ*, 770, 37
- Kitiashvili, I. N., Kosovichev, A. G., Mansour, N. N., & Wray, A. A. 2011, *ApJL*, 727, L50
- Kitiashvili, I. N., Kosovichev, A. G., Mansour, N. N., Lele, S. K., & Wray, A. A. 2012, *Phys. Scr.*, 86, 018403
- Lemen, J. R., Title, A. M., Akin, D. J., et al. 2012, *Sol. Phys.*, 275, 17
- Li, X., Morgan, H., Leonard, D., & Jeska, L. 2012, *ApJL*, 752, L22
- Moll, R., Cameron, R. H., & Schüssler, M. 2011, *A&A*, 533, A126
- Moll, R., Cameron, R. H., & Schüssler, M. 2012, *A&A*, 541, A68
- Nordlund, A. 1985, *Sol. Phys.*, 100, 209
- Orozco Suárez, D., Asensio Ramos, A., & Trujillo Bueno, J. 2012, *ApJL*, 761, L25
- Porter, D. H. & Woodward, P. R. 2000, *ApJS*, 127, 159
- Scharmer, G. B., Bjelksjo, K., Korhonen, T. K., Lindberg, B., & Petterson, B. 2003, in *Society of Photo-Optical Instrumentation Engineers (SPIE) Conference Series*, ed. S. L. Keil & S. V. Avakyan, Vol. 4853, 341
- Shelyag, S., Cally, P. S., Reid, A., & Mathioudakis, M. 2013, *ApJL*, 776, L4
- Skartlien, R., Stein, R. F., & Nordlund, Å. 2000, *ApJ*, 541, 468
- Steiner, O., Franz, M., Bello González, N., et al. 2010, *ApJL*, 723, L180
- Steiner, O. & Rezaei, R. 2012, in *Astronomical Society of the Pacific Conference Series*, Vol. 456, *Fifth Hinode Science Meeting*, ed. L. Golub, I. De Moortel, & T. Shimizu, 3
- Su, Y. & van Ballegoijen, A. 2013, *ApJ*, 764, 91
- Su, Y., Wang, T., Veronig, A., Temmer, M., & Gan, W. 2012, *ApJL*, 756, L41
- Vargas Domínguez, S., Palacios, J., Balmaceda, L., Cabello, I., & Domingo, V. 2011, *MNRAS*, 416, 148
- Vögler, A., Shelyag, S., Schüssler, M., et al. 2005, *A&A*, 429, 335
- Wedemeyer, S., Freytag, B., Steffen, M., Ludwig, H.-G., & Holweger, H. 2004, *A&A*, 414, 1121
- Wedemeyer, S., Scullion, E., Rouppe van der Voort, L., Bosnjak, A., & Antolin, P. 2013a, *ApJ*, 774, 123
- Wedemeyer, S., Scullion, E., Steiner, O., de la Cruz Rodríguez, J., & Rouppe van der Voort, L. H. M. 2013b, *Journal of Physics Conference Series*, 440, 012005
- Wedemeyer-Böhm, S. & Rouppe van der Voort, L. 2009, *A&A*, 507, L9
- Wedemeyer-Böhm, S., Scullion, E., Steiner, O., et al. 2012, *Nature*, 486, 505
- Yan, X. L., Pan, G. M., Liu, J. H., et al. 2013, *AJ*, 145, 153
- Zhou, J., Adrian, R. J., Balachandar, S., & Kendall, T. M. 1999, *Journal of Fluid Mechanics*, 387, 353